

## Photophysical and Photochemical Properties of W(0) and Re(I) Carbonyl Complexes Incorporating Ferrocenyl-Substituted Pyridine Ligands

Shih-Sheng Sun, Dat T. Tran, Onduru S. Odongo, and Alistair J. Lees\*

Department of Chemistry, State University of New York at Binghamton, Binghamton, New York 13902-6016

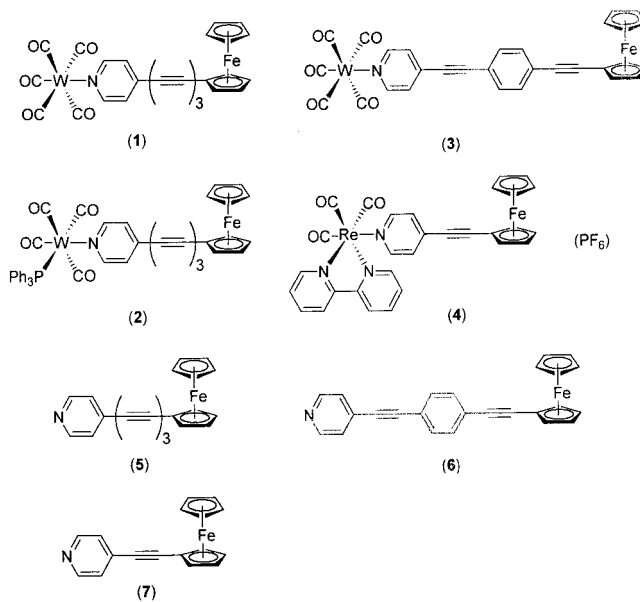
Received July 5, 2001

## Introduction

Complexes of polypyridyl d<sup>6</sup>-metal (W<sup>0</sup> and Re<sup>I</sup>) carbonyl complexes have received a great deal of attention because of their relatively straightforward synthetic procedures and their intriguing photophysical, photochemical, and electrochemical properties.<sup>1</sup> Ferrocene and its derivatives have been studied for their mixed-valence,<sup>2</sup> charge-transfer,<sup>3</sup> and electrochemical properties;<sup>3a,4</sup> their special redox-active features have also been used to develop electrochemical sensors.<sup>5</sup> However, while most of these studies are focused on homonuclear ferrocenes bridged by different organic spacers,<sup>6</sup> the incorporation of a ferrocene moiety within metal carbonyl complexes has been investigated much less.<sup>7</sup> A few studies have appeared which have primarily focused on the synthesis, electrochemistry, and potential application as nonlinear optical materials of such species,<sup>7</sup> but investigations of their photophysical and photochemical properties are lacking.<sup>8</sup>

In this paper, we report the photophysical and photochemical properties of several polypyridyl d<sup>6</sup>-metal (W<sup>0</sup> and Re<sup>I</sup>) carbonyl complexes incorporating ferrocene end-capped pyridine ligands. The structures of these complexes and ligands are illustrated in Chart 1.

Chart 1



## Experimental Section

**Materials.** Complexes 1–4 (see Chart 1) were prepared according to published procedures.<sup>6,7a</sup> Other chemicals were commercially available and used as received.

**General Procedures and Methods.** UV–vis spectra were obtained using a HP 8450A diode array spectrophotometer. Emission spectra were recorded in deoxygenated solvent solution at 293 K with an SLM 48000S lifetime fluorescence spectrophotometer equipped with a red sensitive Hamamatsu R928 photomultiplier tube. The emission lifetimes were collected on a PRA system 300 time-correlated pulsed single-photon apparatus or using a Laser Photonics nitrogen laser as the excitation source (337 nm) and a Tektronix TDS 544A digitizer for decay data acquisition. The obtained lifetimes were fitted to a single-exponential decay in each case (PRA system software version 3.0 or Sigma plot version 4.0) and found to be reproducible to within 5%. The average  $\chi^2$  was less than 1. Detailed procedures for luminescence and lifetime experiments have been described in previous papers.<sup>9</sup> Irradiations at 405 and 428 nm were carried out with light from an Oriel

\* Author to whom correspondence should be addressed. E-mail: alees@binghamton.edu.

- (1) (a) Lees, A. J. *Chem. Rev.* **1987**, *87*, 711. (b) Geoffroy, G. L.; Wrighton, M. S. *Organometallic Photochemistry*; Academic Press: New York, 1979.
- (2) (a) Liu, T.-Y.; Chen, Y. J.; Tai, C.-C.; Kwan, K. S. *Inorg. Chem.* **1999**, *38*, 674. (b) Díaz, C.; Arancibia, A. *Inorg. Chim. Acta* **1998**, *269*, 246.
- (3) (a) Zhu, Y.; Wolf, M. O. *J. Am. Chem. Soc.* **2000**, *122*, 10121. (b) Mata, J. A.; Uriel, S.; Llusar, R.; Peris, E. *Organometallics* **2000**, *19*, 3797. (c) Oldenburg, K.; Vogler, A. *J. Organomet. Chem.* **1997**, *544*, 101.
- (4) Allgeier, A. M.; Mirkin, C. A. *Angew. Chem., Int. Ed.* **1998**, *37*, 894.
- (5) Beer, P. D.; Gale, P. A.; Chen, G. Z. *J. Chem. Soc., Dalton Trans.* **1999**, 1897.
- (6) Lin, J. T.; Wu, J. J.; Li, C.-S.; Wen, Y. S.; Lin, K.-J. *Organometallics* **1996**, *15*, 5028.
- (7) (a) Lin, J. T.; Sun, S.-S.; Wu, J. J.; Liaw, Y. C.; Lin, K.-J. *J. Organomet. Chem.* **1996**, *517*, 217. (b) Lin, J. T.; Sun, S.-S.; Wu, J. R.; Lee, L.; Lin, K.-J.; Huang, Y. F. *Inorg. Chem.* **1995**, *34*, 2323. (c) Yeung, L. K.; Kim, J. E.; Chung, Y. K.; Rieger, P. H.; Sweigart, D. A. *Organometallics* **1996**, *15*, 3891. (d) Kotz, J. C.; Nivert, C. L.; Lieber, J. M.; Reed, R. C. *J. Organomet. Chem.* **1975**, *91*, 87.
- (8) (a) Miller, T. M.; Ahmed, K. J.; Wrighton, M. S. *Inorg. Chem.* **1989**, *28*, 2347. (b) Thomas, K. R. J.; Lin, J. T.; Lin, H.-M.; Chang, C.-P.; Chuen, C.-H. *Organometallics* **2001**, *20*, 557.

- (9) (a) Sun, S.-S.; Lees, A. J. *J. Am. Chem. Soc.* **2000**, *122*, 8956. (b) Wang, Z.; Lees, A. J. *Inorg. Chem.* **1993**, *32*, 1493.

**Table 1.** Absorption and Emission Data

compd	absorption <sup>a</sup>				emission			
	$\lambda_{\max}$ , nm ( $\epsilon \times 10^{-3}$ , M <sup>-1</sup> cm <sup>-1</sup> )	$\lambda_{\text{em}}$ , nm	$\Phi_{\text{em}}$	$\tau$ , ns	$k_r$ , s <sup>-1</sup>			
<b>1</b> <sup>b</sup>	229 (74.9), 243 (75.8), 284 (31.0), 328 (14.6), 361 (16.6), 397 (18.6), 502 (sh, 5.1)	472	<10 <sup>-4</sup>	32	<3.1 × 10 <sup>3</sup>			
<b>2</b> <sup>b</sup>	255 (64.8), 289 (sh, 37.8), 347 (14.5), 464 (12.7)	560	<10 <sup>-4</sup>	27	<3.7 × 10 <sup>3</sup>			
<b>3</b> <sup>b</sup>	230 (68.8), 326 (35.1), 390 (23.3)	494	<10 <sup>-4</sup>	35	<2.9 × 10 <sup>3</sup>			
<b>4</b> <sup>c</sup>	250 (27.8), 262 (27.9), 314 (30.0), 319 (31.8), 336 (sh, 23.4), 390 (5.7), 470 (2.7)	562	1.8 × 10 <sup>-3</sup>	132	1.4 × 10 <sup>4</sup>			

<sup>a</sup> Deoxygenated CH<sub>3</sub>CN solution at 293 K. <sup>b</sup> The emission was measured in EPA at 77 K.  $\lambda_{\text{ex}} = 400$  nm. <sup>c</sup> The emission was measured in deoxygenated CH<sub>3</sub>CN solution at 293 K.  $\lambda_{\text{ex}} = 370$  nm.

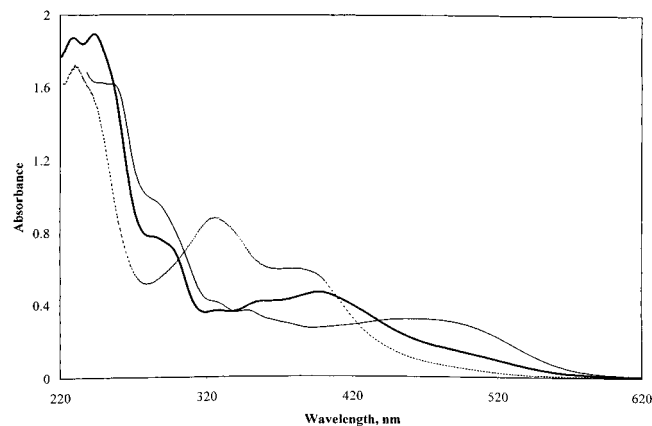


**Figure 1.** Electronic absorption spectra at 293 K of  $2.5 \times 10^{-5}$  M complexes **1** (bold line, —), **2** (light line, —), and **3** (---) in CH<sub>3</sub>CN.

Instruments 450-W mercury arc lamp using interference filters (Ealing Corp., 10-nm band-pass) to isolate the excitation wavelength. Typical light intensity was  $5 \times 10^{-8}$  to  $1 \times 10^{-7}$  einstein/min. A Lexel Corp. model 95-4 argon ion laser (4 W all lines) was used to perform the photolysis at 458, 488, and 514 nm with typical laser powers of between 20 and 30 mW. The photochemical quantum efficiencies were calculated on the basis of the first 40% conversion of the reaction, and the errors were found to be within 10% (with quantum efficiencies above  $10^{-6}$ ). Detailed procedures for the photolysis experiments and the calculation of the photochemical quantum yield have been described in previous papers.<sup>10</sup>

## Results and Discussion

Electronic absorption spectral data obtained for **1–4** are summarized in Table 1. Figure 1 illustrates the absorption spectra of **1–3** in CH<sub>3</sub>CN at 293 K. The absorption spectra of **1–3** display a series of high-energy absorption bands below 360 nm, which are assigned to the  $\pi-\pi^*$  transitions localized on the pyridine ligands.<sup>6</sup> The lowest energy absorption bands in **1–3** are assigned to W ( $d\pi$ ) to pyridine ligand ( $\pi^*$ ) charge-transfer transitions (MLCT).<sup>6,11</sup> They are in the energy order of **2** (464 nm) < **1** (397 nm) < **3** (390 nm), which is consistent with the weaker  $\pi$  acceptor nature of PPh<sub>3</sub> compared to CO and the lower amount of conjugation in ligand **6** compared to ligand **5**. The less intense ligand field (LF) bands from the W(0) center are significantly convoluted with the intense  $\pi-\pi^*$  and MLCT transitions, and their exact energy positions are not specifically identified.<sup>1,11,12</sup>

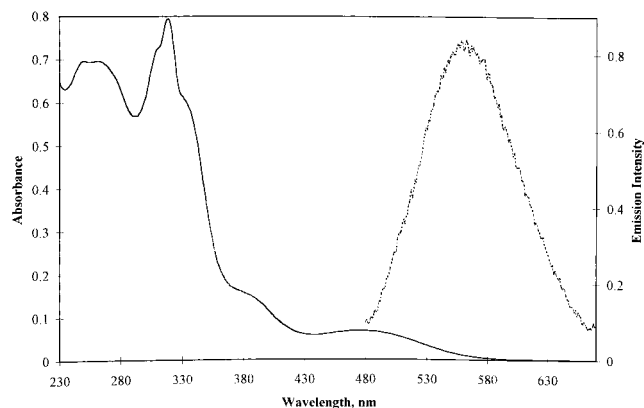


**Figure 2.** Electronic absorption (—) and emission (···) spectra of complex **4** at 293 K.

Complexes **1–3** do not exhibit room-temperature emission and only show very weak emission in 77 K glasses in the 470–560 nm region with quantum yields less than  $10^{-4}$ . The emission maxima and lifetimes of complexes **1–3** at 77 K are also listed in Table 1. The broad, structureless emission is assigned to the <sup>3</sup>MLCT transition, and the emission maxima from the complexes are in the energy order of **2** (560 nm) < **3** (494 nm) < **1** (472 nm). The lower energy emission band position of **3** compared to **1** is rationalized on the basis that the benzene ring in ligand **6** of the complex is distorted in the excited state in a way that maximizes the  $\pi$  electron conjugation, thereby lowering the energy of the  $\pi^*$  orbital.<sup>12</sup> Alternatively, the reordering of the excited-state energy may arise from the contribution of reorganization energy.<sup>13</sup> It is noticeable that the lifetimes of complexes **1–3** do not vary much as they are each in the range 27–35 ns. However, the relatively slow radiative decay process ( $k_r$ ) indicates that the intramolecular energy transfer from the <sup>3</sup>MLCT state to the excited state of the ferrocene moiety is highly efficient in each of complexes **1–3**, even at 77 K.

Figure 2 shows the absorption and emission spectra of **4** in deoxygenated CH<sub>3</sub>CN solution at 293 K. Excitation of complex **4** at 337 nm generates an emission maximum at 562 nm with a single-exponential decay lifetime of 132 ns. In addition, the reduction potentials of complex **4** show that the bpy-based first reduction potential is significantly lower than the ligand **7** based reduction potentials.<sup>7a</sup> On the basis of the structureless emission spectral profile, long lifetime, and the reduction potentials, we tentatively assign this

(10) (a) Dunwoody, N.; Sun, S.-S.; Lees, A. J. *Inorg. Chem.* **2000**, *39*, 4442. (b) Lees, A. J. *Anal. Chem.* **1996**, *68*, 226.

(11) Lees, A. J.; Fobare, J. M.; Mattimore, E. F. *Inorg. Chem.* **1984**, *23*, 2709.

(12) (a) Zulu, M. M.; Lees, A. J. *Inorg. Chem.* **1988**, *27*, 1139. (b) Manuta, D. M.; Lees, A. J. *Inorg. Chem.* **1986**, *25*, 1354.

(13) Chen, P.; Meyer, T. J. *Chem. Rev.* **1998**, *98*, 1439.

## NOTE

**Table 2.** Wavelength Dependence of Photosubstitution Quantum Yields in  $\text{CH}_2\text{Cl}_2$  at 293 K<sup>a</sup>

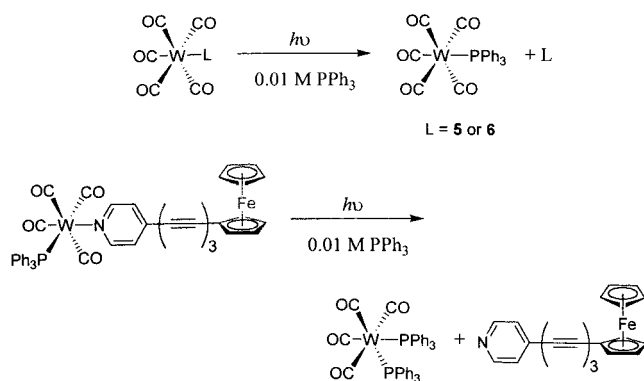
complex	405 nm $10^3\Phi_{\text{cr}}$	428 nm $10^3\Phi_{\text{cr}}$	458 nm $10^5\Phi_{\text{cr}}$	488 nm $10^5\Phi_{\text{cr}}$	514 nm $10^5\Phi_{\text{cr}}$
<b>1</b>	17	5.1	13	4.0	0.81
<b>2</b>	2.5	1.6	3.1	1.1	0.53
<b>3</b>	27	6.5	31	0.82	<i>b</i>

<sup>a</sup> Photolysis performed in deoxygenated solution of  $\sim 4 \times 10^{-5}$  M complex containing 0.01 M  $\text{PPh}_3$  as entering ligand. <sup>b</sup> The complex absorbs insufficiently at 514 nm to obtain an accurate quantum yield.

emission band to the triplet  $d\pi$  (Re) to  $\pi^*$  (bpy) CT transition. Although a single-exponential decay of the emissive excited state was observed in complex **4**, the possibility of a fast equilibrium between the bpy-based  $^3\text{MLCT}$  and ligand **7** based  $^3\text{MLCT}$  states cannot be completely ruled out. The relatively low emission quantum yield and shorter lifetime of **4** compared to  $(\text{bpy})\text{Re}(\text{CO})_3(4\text{-Etpy})\text{-}(\text{PF}_6)$  ( $\Phi_{\text{em}} = 0.027$  and  $\tau = 218$  ns)<sup>14</sup> is attributed to the presence of low-lying nonemissive LF excited states localized on ferrocene with the possible involvement of a ligand-to-ligand (ferrocene to bpy) charge-transfer (LLCT) excited state.<sup>15</sup> Some recent studies on rhenium(I) carbonyl systems have indicated that low-lying intraligand (IL) states<sup>16</sup> or ligand-to-ligand charge transfer (LLCT) states<sup>17</sup> are competitive in excited-state energy relaxation processes with the lowest energy MLCT state. The participation of these excited states would largely account for the decreasing emission quantum yields and shorter lifetimes of the emissive  $^3\text{MLCT}$  excited states.

Photosubstitution quantum efficiencies of complexes **1–3** upon photolysis in the presence of excess  $\text{PPh}_3$  as entering ligand are collected in Table 2. It was observed that the MLCT band slowly decreased with an increasing irradiation period. By comparing the IR and UV–vis absorption spectra of the photolysis products to literature values,<sup>6,18</sup> we can conclude that the irradiation of complexes **1–3** in the presence of excess scavenging ligand in solution is the consequence of the dissociation of the pyridine ligands. Scheme 1 illustrates the reactions that occur upon photoexcitation

**Scheme 1**<sup>a</sup>



<sup>a</sup>  $\lambda = 405, 428, 458, 488,$  and  $514$  nm.

for complexes **1–3**. The formation of  $(\text{CO})_5\text{W}(\text{PPh}_3)$  instead of  $(\text{CO})_4\text{W}(\text{PPh}_3)(\text{L})$  for complexes **1** and **3** and the formation

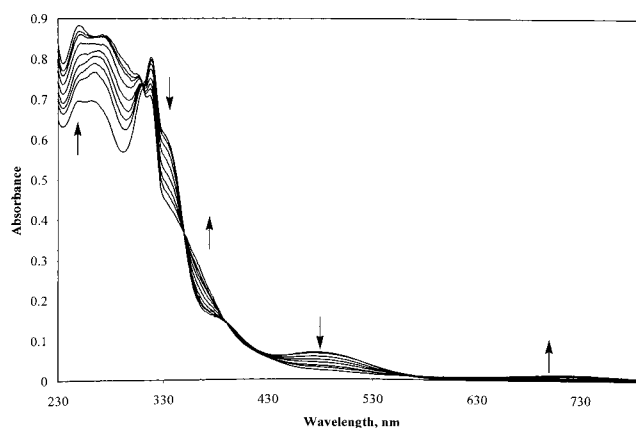


**Figure 3.** Spectrophotometric titration curves of complex **4** by Ce(IV) in  $\text{CH}_3\text{CN}$  solution.

of  $(\text{CO})_4\text{W}(\text{PPh}_3)_2$  instead of  $(\text{OC})_3\text{W}(\text{PPh}_3)_2(\text{L})$  for complex **2** indicate the labilization of the weak-field pyridine ligand following  $^1\text{A}_1(\text{e}^4\text{b}_2^2) \rightarrow ^1\text{E}(\text{e}^3\text{b}_2^2\text{a}_1^1)$  excitation.<sup>1,12,18a</sup> The observed wavelength-dependent photochemical quantum efficiencies, which decrease with lower energy excitation, are consistent with the model of a reactive  $^3\text{LF}$  state lying above the unreactive  $^3\text{MLCT}$  state.<sup>12</sup> Complex **4** shows no photochemical reactivity under the same experimental conditions. The lack of spectroscopically accessible LF bands in complex **4** is associated with this photochemical inertness.

Notably, Wrighton and co-workers have reported the observation of a ligand-to-metal charge transfer (LMCT) band from the oxidized ferrocenium ion when they performed controlled-potential electrolysis of a series of ferrocenylphosphine-coordinated rhenium(I) tricarbonyl complexes.<sup>8a</sup> In addition, Oldenburg and Vogler have observed this LMCT band from the ferrocenium moiety in complex  $(\text{dppf})\text{Re}(\text{CO})_3\text{Cl}$  where dppf is 1,1'-bis(diphenylphosphino)ferrocene.<sup>3c</sup> UV–vis spectral traces of complexes **1–4** were recorded during their titration with oxidizing reagent ammonium cerium(IV) nitrate. In each of complexes **1–3**, the addition of Ce(IV) bleaches the MLCT band and it also causes a slow decomposition reaction. However, in contrast, there is no sign of decomposition for complex **4** during the titration. The spectrophotometric titration curves obtained from complex **4** in  $\text{CH}_3\text{CN}$  solution are displayed in Figure 3. It is clear that there are a series of isosbestic points (311, 351, 393, 426, and 584 nm) in the spectral traces from **4**. In particular, a low-energy band at 722 nm appears which has an extinction coefficient of  $552 \text{ M}^{-1} \text{ cm}^{-1}$ ; this is characteristic of the ferrocenium ion.<sup>19</sup>

- (15) Extended Hückel calculation derived from CAChe 3.8 shows that the HOMO is a Fe-centered MO and LUMO is a bpy-centered MO. In addition, the very low oxidation potential of  $\text{Fe}^{2+}$  in ligand **7**<sup>a</sup> also provides the possible existence of a low-energy emission-silent LLCT state in complex **4**.
- (16) (a) Ferraudi, G.; Feliz, M.; Wolcan, E.; Hsu, I.; Moya, S. A.; Guerrero, J. J. *Phys. Chem.* **1995**, *99*, 4929. (b) Guerrero, J.; Piro, O. E.; Feliz, M. R.; Ferraudi, G.; Moya, S. A. *Organometallics* **2001**, *20*, 2842.
- (17) (a) Schanze, K. S.; MacQueen, D. B.; Perkins, T. A.; Cabana, L. A. *Coord. Chem. Rev.* **1993**, *122*, 63. (b) Liard, D. J.; Vlcek, A. *Inorg. Chem.* **2000**, *39*, 485.
- (18) (a) Dahlgren, R. M.; Zink, J. I. *Inorg. Chem.* **1977**, *16*, 3154. (b) Mathieu, R.; Poilblanc, R. *Inorg. Chem.* **1972**, *11*, 1858.
- (19) Sohn, Y. S.; Hendrickson, D. N.; Gray, H. B. *J. Am. Chem. Soc.* **1971**, *93*, 3603.

(14) Tapolsky, G.; Duesing, R.; Meyer, T. J. *Inorg. Chem.* **1990**, *29*, 2285.

Accompanying these changes in the absorption spectra, the infrared CO stretching frequencies are also shifted to higher frequencies although to somewhat different extents. This observation is expected as the oxidized ferrocenium moiety is more electron-withdrawing than a neutral ferrocene moiety and, thus, this reduces the amount of  $\pi$  back-bonding from the metal to the CO ligands.<sup>4,7d,8a</sup> The order of the average CO frequency shift on oxidation is **3** ( $1\text{ cm}^{-1}$ )  $\sim$  **4** ( $1\text{ cm}^{-1}$ )  $<$  **1** ( $5\text{ cm}^{-1}$ )  $<$  **2** ( $11\text{ cm}^{-1}$ ). While complexes **3** and **4** exhibit no significant shift in CO frequencies, complexes **1** and **2** do show appreciable frequency shifts, which reflects the stronger interaction between the ferrocene moiety and the metal center. In the case of complex **4**, the positively charged Re(I) atom seems to neutralize the effect from the oxidation of ferrocene as this complex has the shortest separation between the Re(I) and ferrocene moieties. In the case of complex **3**, the lack of planarity between the phenyl ring and pyridine ring, as evidenced in its solid-state

structure<sup>6</sup> as well as the highest energy MLCT transition among complexes **1–3**, is attributed to the small shift in CO frequencies.

**Acknowledgment.** We are grateful to the Division of Chemical Sciences, Office of Basic Energy Sciences, Office of Science, U.S. Department of Energy (Grant DE-FG02-89ER14039), for support of this research.

**Supporting Information Available:** A figure illustrating a representative spectral sequence obtained upon photolysis at 428 nm of complex **3** in deoxygenated  $\text{CH}_2\text{Cl}_2$  solution containing an excess amount of entering ligand  $\text{PPh}_3$ . A table listing the IR data of photolysis products of complexes **1–3** and a table summarizing the CO stretching frequencies of complexes **1–4** and their oxidized forms. This material is available free of the charge via the Internet at <http://pubs.acs.org>.

IC010713Y